

Soft Maximin Estimation for Heterogeneous Array Data

Adam Lund, Søren Wengel Mogensen, and Niels Richard Hansen*

September 24, 2020

Abstract

The extraction of a common signal across many recordings is difficult when each recording – in addition to the signal – contains large, unique variation components. Maximin estimation has previously been proposed as a robust estimation method in the presence of heterogeneous noise.

We propose soft maximin estimation as a computationally attractive methodology for estimating a common signal from heterogeneous data. The soft maximin loss is introduced as an aggregation, controlled by a parameter $\zeta > 0$, of explained variances and the estimator is obtained by minimizing the penalized soft maximin loss.

By establishing statistical and computational properties we argue that the soft maximin method is a statistically sensible and computationally attractive alternative to existing methods. In particular we demonstrate, on simulated and real data, that the soft maximin estimator can outperform existing methods both in terms of predictive performance and run time.

We also provide a time and memory efficient implementation for data with array-tensor structure in the R package *SMMA* available on CRAN.

heterogeneous data, robust estimation, regularization, convex optimization, array-tensor structure

1 Introduction

We consider a general estimation setup where the objective is to extract a common effect or signal from heterogeneous data. As heterogeneity is particularly prevalent in large-scale settings our focus is on obtaining a computationally attractive estimation methodology that works in those settings. In particular, special attention is given to a setting with array data organized in known groups, from which we seek to retrieve a common signal, i.e. a signal present in all groups. This common signal will typically be dominated or masked by

*University of Copenhagen, Department of Mathematical Sciences, Universitetsparken 5, 2100 Copenhagen Ø, Denmark, e-mail: adam.lund@math.ku.dk (A. Lund).

group specific signals in some or all groups. However, while the paper focuses on this specific setting, the methodology we propose can also be applied in data settings without a known grouping or array structure.

We use a real experimental brain imaging data set to illustrate the setting and in particular to elucidate the concept of a masked common effect (signal) embedded in a heterogeneous data set. Specifically, this data set consists of movies of neuronal activity in ferret brains recorded over experimental trials. The trials naturally lead to a group structure on the data set. Furthermore, in each trial, a visual stimulus is presented to the ferret to elicit a neuronal response signal in the visual cortex. Therefore a response signal, possessing specific features that are similar across all trials, should hypothetically be present in each trial. This set of shared features is then the common signal. However, since the experiment was repeated in each trial for each ferret (13 in total) we also expect heterogeneous features (trial and animal specific) to be present. As such the neuronal data set provides a concrete example of heterogeneous array data with a known group structure, and with an embedded common signal.

On this real data as well as on simulated data we evaluate the predictive performance of the soft maximin methodology by benchmarking it against existing methods. To obtain the predictions we use a linear model with a mean component expressed in a basis expansion that allows us to estimate the common (response) signal. If the mean components across all groups are identical, the common mean component can be interpreted as the common signal and extracted via least squares estimation of the basis coefficient, say. That is, by pooling data across all groups to obtain the pooled least squares estimate. However, if the recordings are heterogeneous in the sense that the mean component cannot be regarded as fixed, pooling the data may lead to overfitting dominant group specific features. Extracting features that are group specific can in turn impact the predictive performance of the estimator adversely.

This is illustrated in Figure 1 where the outcome of using both pooled and soft maximin estimators, to extract a common Gaussian signal from four simulated heterogeneous data sets, is shown. For one data set the pooled estimator is successful in extracting a clear Gaussian signal but it fails on the other three. In contrast the soft maximin estimators ($\zeta = 100, 200$) perform well on all sets and display less variation. Figure 1 also shows the maximin aggregation (magging) estimate, a computationally attractive approximation to the maximin estimator proposed in Bühlmann and Meinshausen (2016).

While explicit modeling of heterogeneity is possible for the data setting we consider, e.g. studied in the field of functional data analysis, Scheipl et al. (2015); Staicu et al. (2010); Wang et al. (2016), we will not pursue this more sophisticated modeling framework. Though heterogeneity may represent structured variation, it may have many different known as well as unknown origins. In the neuronal data temporal heterogeneity can arise across recordings for a single animal due to slightly varying experimental conditions or due to fatigue, and spatial heterogeneity due to differences in the cytoarchitecture. Characterizing and modeling the exact nature of the heterogeneity can be very difficult, and our focus is instead on fast, robust estimation of a common signal.

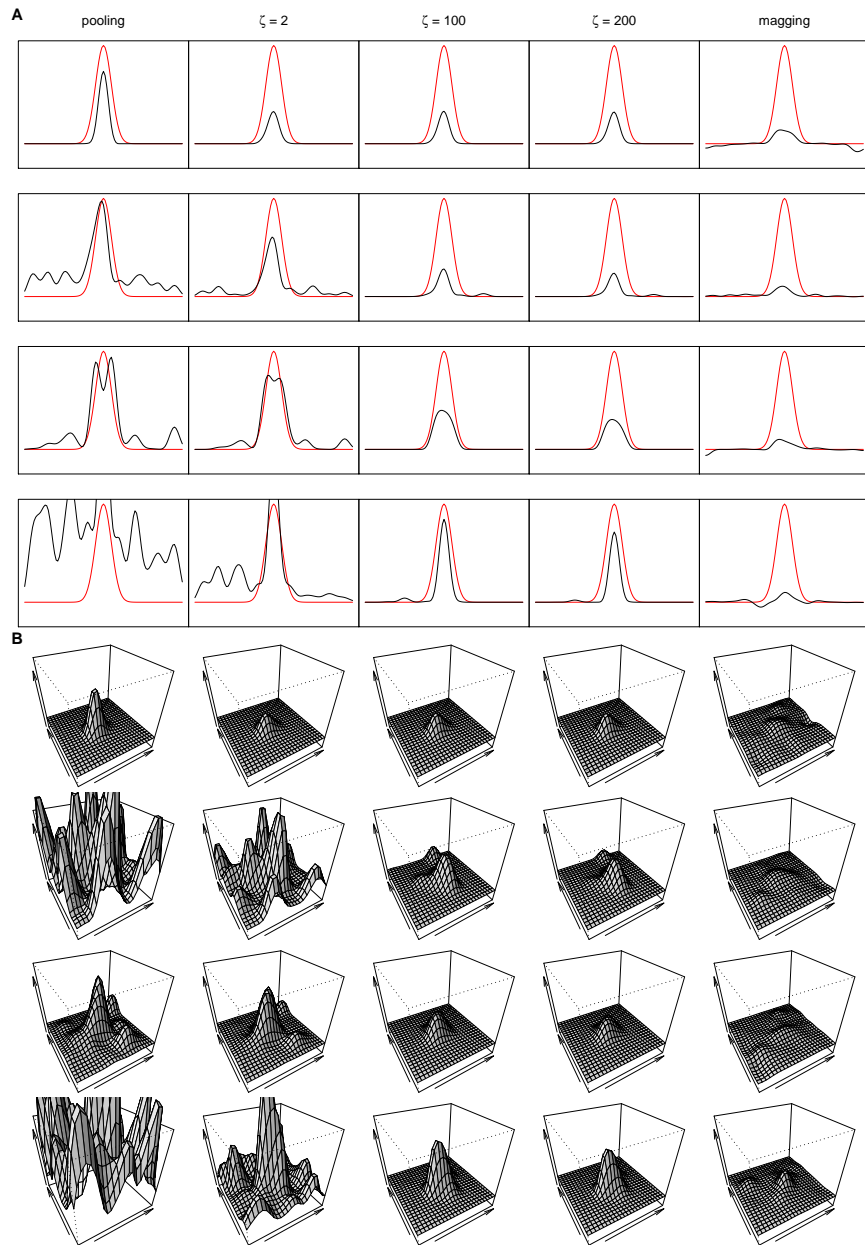


Figure 1: A: Temporal plots obtained when fixing $(x, y) = (12, 12,)$ and plotting the true Gaussian signal $\phi(x, y, t)$ (red) together with the estimated signal $\hat{Y}_{x,y,t}$ (black) for model no. 10. Each column corresponds to a method; pooling, soft maximin with $\zeta = 2, 100, 200$ and magging. Each row corresponds to a training set with 14 groups. B: Spatial plots of the estimates $\hat{Y}_{x,y,t}$ from panel A obtained when fixing $t = 50$.

In Meinshausen and Bühlmann (2015) a maximin approach is proposed as a way to obtain a good, robust and computationally attractive estimator for large-scale heterogeneous data within the framework of linear models. Their population quantity called the maximin effect is the common signal, and they propose to estimate this quantity using families of estimators defined as solutions to convex minimization problems, see (9) in Meinshausen and Bühlmann (2015). These maximin estimators are, however, difficult to compute. Though they are given as solutions to convex minimization problems, the objective functions are always non-differentiable and also non-separable in the sense of Tseng and Yun (2009).

We will argue that the soft maximin estimator is a computationally attractive and statistically sound approximation to the maximin estimator. More importantly, it offers an entire range of estimators of independent interest. Explicitly it works by aggregating explained variances across groups (or more generally convex group divergence functions) using a family of soft maximum functions indexed by a parameter $\zeta > 0$. By controlling ζ we demonstrate that the soft maximin estimator effectively interpolates the pooled estimator and the maximin estimator.

To support that soft maximin estimation is attractive we show that the corresponding loss function is strongly convex under a full rank assumption on the design matrices (strongly convex group divergence functions) and in particular has a Lipschitz continuous gradient when the design is identical across groups. Strong convexity can be used to obtain convergence guarantees and the explicit Lipschitz constant can be used to select an efficient step size. We also compute the performance loss incurred relative to the theoretical maximin effect performance, which depends on the soft maximin parameter ζ . This provides an explicit quantification of the statistical properties of the computationally attractive soft maximin estimator relative to the computationally unattractive maximin estimator.

The resulting algorithm, following Lund et al. (2017), provides a time and space efficient solution algorithm for soft maximin estimation for array data. It is implemented in the R package *SMMA* available from CRAN, Lund (2020).

The paper is organized as follows: The general model and estimation framework is outlined in Section 2 and statistical properties of soft maximin estimation are discussed. In Section 3 we consider computational aspects of soft maximin estimation and propose a solution algorithm for the general soft maximin problem. We also introduce and discuss computational aspects of a specific model for array data. In Section 4, to compare and benchmark soft maximin estimation against existing methods, we carry out numerical experiments on both simulated and real data. Section 5 summarizes the proposed methodology and its relation to alternative methods.

2 Estimation framework

Consider n observations y_1, \dots, y_n with a possible group structure meaning that y_i may have features that it shares with a subset of observations (a group) in addition to observation specific features. Furthermore, some features may be population level features that are shared among all observations in the given data set and can therefore be referred to as common. Such data is heterogeneous in the sense of displaying a hierarchical variation at population level, group level and individual level.

If the group structure is unknown, the inference problem for such data is twofold as it entails simultaneously uncovering an unknown group structure (clustering) as well as estimating the population and group level features.

A general linear *mixture* model, see Meinshausen and Bühlmann (2015), that reflects both these aspects, has the univariate response variables Y_1, \dots, Y_n generated as

$$Y_i = X_i^\top B_i + \varepsilon_i, \quad i = 1, \dots, n. \quad (1)$$

Notably, B_1, \dots, B_n are p -dimensional random variables identically distributed according to an unknown distribution F_B , but not necessarily independent, X_1, \dots, X_n are i.i.d p -dimensional variables with population Gram matrix Σ and ε_i is an appropriate noise term.

The data heterogeneity in this model arises as a consequence of the variation in B_i as governed by F_B . Note that this model setup encompasses situations without any group structure. This for instance happens if the model parameters captures a smoothly varying effect over an ordered index i , e.g. a time-varying coefficient model. To capture a smoothly varying effect, F_B must have continuous support and in particular no true grouping of observations exists since every B_i is unique.

Here we present the methodology in a setup with a known group structure such that the effects B_i are constant within each group. This in turn implies a finite support for F_B and the model is then perhaps better understood as a type of linear *mixed* model since the clustering or grouping is available hence no longer part of the inference. In contrast to a traditional mixed model, however, we avoid explicitly modeling fixed and random effects since the aim is not to draw inference about these. Instead we seek to obtain only an estimate of the possible common effects present in the data.

Note that while the estimation methodology is most easily introduced in a setup with known groups, by adopting a set of structural assumptions, it can also be applied in the more general setting, with unknown or no existing group structure, by explicitly constructing a group structure on the observations, as detailed in Meinshausen and Bühlmann (2015).

2.1 Soft maximin estimation with known groups

To introduce $G \in \mathbb{N}$ groups in the setup above, suppose given a partition I_1, \dots, I_G of the index set $\{1, \dots, n\}$ such that $|I_g| = n_g$, and $n = \sum_g n_g$ where

for each g and for all $i \in I_g$, $B_i = B_g$ is the effect in group g . Thus F_B has finite unknown support with cardinality G , that is $\text{supp}(F_B) = \{b_1, \dots, b_G\} \subset \mathbb{R}^p$ with $b_g := B_g(\omega)$ the true unknown effect in group g .

Using this extra structure we can label the response, covariates and errors according to group. For the g th group let $\mathbf{Y}_g = (Y_{g,1}, \dots, Y_{g,n_g})^\top$ be the $n_g \times 1$ response vector, $\mathbf{X}_g = (X_{g,1} | \dots | X_{g,n_g})^\top$ the $n_g \times p$ design matrix, and $\boldsymbol{\varepsilon}_g = (\varepsilon_{g,1}, \dots, \varepsilon_{g,n_g})^\top$ the $n_g \times 1$ error vector. The linear model for the g th group is then

$$\mathbf{Y}_g = \mathbf{X}_g b_g + \boldsymbol{\varepsilon}_g, \quad g \in \{1, \dots, G\}. \quad (2)$$

A *common signal* in this framework is represented by a single $\beta \in \mathbb{R}^p$ such that $\mathbf{X}_g \beta$ is a good and robust approximation of $\mathbf{X}_g b_g$ across all G groups.

To gauge the quality of the approximation we adopt the optimality criterion from Meinshausen and Bühlmann (2015). There the explained variance in group g when using some $\beta \in \mathbb{R}^p$ in (2) is defined as

$$V_{b_g}(\beta) := 2\beta^\top \Sigma b_g - \beta^\top \Sigma \beta. \quad (3)$$

The optimal approximation across all groups is then the so-called maximin effect defined as a $b^* \in \mathbb{R}^p$ that maximizes the minimum of the explained variances across groups, i.e. $b^* := \arg \max_\beta \min_g V_{b_g}(\beta)$.

Since b_g is unknown, to make this criteria operational, let $\hat{\Sigma}_g := \mathbf{X}_g^\top \mathbf{X}_g / n_g$ denote the empirical Gram matrix in group g . By (2) replacing Σ with $\hat{\Sigma}_g$ in (3) we obtain the empirical explained variance in group g

$$\hat{V}_g(\beta) := \frac{1}{n_g} (2\beta^\top \mathbf{X}_g^\top \mathbf{Y}_g - \beta^\top \mathbf{X}_g^\top \mathbf{X}_g \beta). \quad (4)$$

The maximin effects estimator is obtained by maximizing (the penalized) minimum of (4) or equivalently by minimizing (the penalized) maximin loss function $\beta \mapsto \max_g \{-\hat{V}_g(\beta)\}$, see (21) in Section 5.

As shown in Meinshausen and Bühlmann (2015) the use of this estimator can lead to more robust estimates for heterogeneous data compared to an estimator that does not take grouping into account i.e. a pooled estimator. The intuition is that the maximin estimator extracts only features that are active with the same sign across groups while setting group specific features to zero. This makes it a more crude estimator compared to one obtained using the full mixed model methodology, however it is in principle also more robust and in particular computationally more attractive.

In large scale data settings, where you typically encounter data heterogeneity, the computational aspect of the estimator is crucial. However, since the max-function is non-differentiable and non-separable the maximin problem (21) is not easy to solve.

We address this computational hurdle by replacing the max-function with the following smooth function. For $G \in \mathbb{N}$ and $\zeta \neq 0$ consider the scaled log-

sum exponential function

$$\text{lse}_\zeta(x) := \frac{\log(\sum_j e^{\zeta x_j})}{\zeta}, \quad x \in \mathbb{R}^G. \quad (5)$$

Clearly lse_ζ is differentiable and as we show in Section 3 it has additional properties that makes it well suited for optimization purposes. First, the basic properties stated next are easily verified (see the appendix) and highlights why (5) is a sensible choice as an approximation of the max-function.

Lemma 1. *Let $G \in \mathbb{N}$ and $x \in \mathbb{R}^G$.*

i) *For $\zeta > 0$ it holds that*

$$\max\{x_1, \dots, x_G\} \leq \text{lse}_\zeta(x) \leq \frac{\log(G)}{\zeta} + \max\{x_1, \dots, x_G\}, \quad (6)$$

and in particular $\text{lse}_\zeta(x) \searrow \max_g\{x_g\}$ as $\zeta \rightarrow \infty$.

ii) *For $\zeta \rightarrow 0$ it holds that*

$$\text{lse}_\zeta(x) = \frac{1}{G} \sum_{j=1}^G x_j + \frac{\log(G)}{\zeta} + o(1).$$

We define the soft maximin loss function, by

$$s_\zeta(\beta) := \text{lse}_\zeta(-\hat{V}(\beta)), \quad \beta \in \mathbb{R}^p, \quad \zeta > 0,$$

where $\hat{V}(\beta) := (\hat{V}_1(\beta), \dots, \hat{V}_G(\beta))^\top$. For $\kappa > 0$ and $\zeta > 0$, the soft maximin estimator can now be defined by

$$\hat{\beta}_{smm}^\kappa := \arg \min_{\beta} \text{lse}_\zeta(-\hat{V}(\beta)) \quad \text{s.t.} \quad \|\beta\|_1 \leq \kappa. \quad (7)$$

Using Lemma 1, it is possible to quantify the impact of the parameter ζ on the performance of the soft maximin estimator (7). The following result gives a bound on the maximum negative explained variance of the soft maximin estimator, using that of the theoretical maximin effect b^* .

Proposition 1. *Let $D = \max_g \|\hat{\Sigma}_g - \Sigma\|_\infty$ and $\delta = \max_g \|\mathbf{X}_g^\top \boldsymbol{\varepsilon}_g / n_g\|_\infty$. For fixed $\zeta > 0$ and $\kappa > 0$, if $\kappa \geq \max_g \|b_g\|_1$,*

$$\max_g \{-V_{b_g}(\hat{\beta}_{smm}^\kappa)\} \leq \max_g \{-V_{b_g}(b^*)\} + 6D\kappa^2 + 4\kappa\delta + \frac{\log(G)}{\zeta},$$

where b^ is the maximin effect. In particular*

$$\|\hat{\beta}_{smm}^\kappa - b^*\|_\Sigma \leq 6\kappa^2 D + 4\kappa\delta + \frac{\log(G)}{\zeta}.$$

Proposition 1 is shown by combining Lemma 1 and results in Meinshausen and Bühlmann (2015), see the appendix. In particular, the performance loss incurred when using the soft maximin estimator is bounded by the same quantity as that of the maximin estimator plus the soft maximum approximation bias $\log(G)/\zeta$ from Lemma 1. Thus the soft maximin estimator enjoys theoretical properties similar to those of the (hard) maximin estimator, when controlling for the parameter ζ . In particular, for $D = 0$ (e.g. for a fixed design) and a fixed number of groups, if $n_g \rightarrow \infty$ for all g , the soft maximin estimator only retains the approximation bias.

Proposition 1 establishes a connection between the soft maximin performance and the maximin effect and shows that for $\zeta \uparrow \infty$ we indeed obtain the maximin estimator performance. However, it also highlights that for $\zeta \downarrow 0$ the performance of the soft maximin estimator can stray arbitrarily far away from that of the maximin estimator. To shed light on this note that by Lemma 1, for small $\zeta > 0$,

$$s_\zeta(\beta) \approx \frac{1}{G} \sum_{j=1}^G -\hat{V}_j(\beta) + \frac{\log(G)}{\zeta} \propto \frac{1}{n} \sum_{j=1}^G \sum_{i=1}^{n_j} \frac{n}{G n_j} ((X_j \beta)_i - Y_{j,i})^2$$

and (7) effectively becomes a penalized weighted least squares (PWLS) problem over all n observations. Thus solving (7) for small $\zeta \geq 0$ approximately yields the pooled PWLS estimator with weights amplifying observations from smaller than average groups. With the same number of observations in each group, the soft maximin estimator in turn interpolates the pooled PLS estimator and the maximin estimator.

In this sense ζ reflects the heterogeneity in the data. If there is little heterogeneity a low or even zero ζ might work well corresponding to grouping not being relevant. However, for heterogeneous data a low ζ might lead to predictions that are worse than the zero prediction, whereas a high ζ can still work well, see Figure 1 and Section 4.

To illustrate the interpolation, consider a small data example with data generated according to (2) with $G = 20$ groups, $n_g = 400$ observations in each group, and a two-dimensional parameter space. For fixed effects $\{b_1, \dots, b_{20}\} \subset \mathbb{R}^2$ we sample X_g and ε_g , $M = 10$ times for each g resulting in 10 different data sets. For each of these ten small data sets we can compute the unpenalized softmaximin estimate (i.e. $\kappa = \infty$ in (7)) for a sequence of ζ values as well as the corresponding maximin estimate (i.e. $\lambda = 0$ in (21)) using base functionality in R. We also compute the pooled population LS estimate and the 20 group LS estimates that we maximin aggregate to obtain the (unpenalized) magging estimate.

Figure 2 displays the interpolation path of the softmaximin estimator connecting the population LS estimates and the maximin estimates. It also shows the group LS estimates and the corresponding maximin aggregated (magging) estimates. Note that all maximin type estimates are clustered around the theoretical maxmin effect indicated with a \blacktriangle on the edge of the convex hull of $\{b_1, \dots, b_{20}\}$ while the pooled estimates are well inside the convex hull.

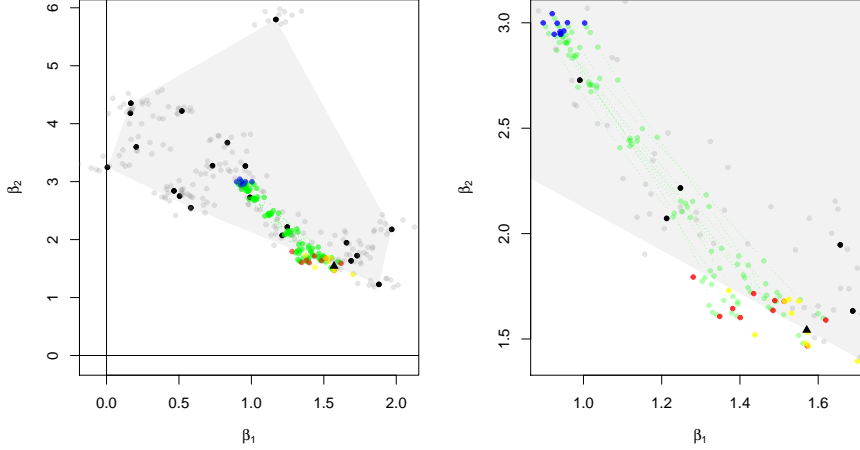


Figure 2: Left: Convex hull (grey shaded area) of $\text{supp } F_B$ (black points). Theoretical maximin effect b^* (\blacktriangle), maximin estimates (red points), soft maximin estimates (green points) for various ζ , magging estimates (yellow points), population LS estimates (blue points) and group LS estimates (grey points). Right: Close up.

We end this section by noting that the application of the soft maximin estimator is not restricted to the known group setting presented here. To apply the soft maximin estimator in a general setup with unknown groups we can, under certain structural assumptions, use random sampling to obtain the index sets I_1, \dots, I_G i.e. a grouping of the data, and then use the methodology as described. This is detailed in Meinshausen and Bühlmann (2015), and in addition to mathematical complexity, adds a layer of substantial computational complexity to the inference procedure since the number of groups G is then a hyperparameter that needs to be inferred e.g. by cross validation. This clustering layer only amplifies the importance of an efficiently computable base estimator.

3 Computational properties

Here we shall consider a general estimation setup where the empirical explained variance $-\hat{V}_g$ from (4) is replaced by a general convex group divergence function, $h_g : \mathbb{R}^p \rightarrow \mathbb{R}$. Particularly, in parallel to the Bregman divergence let $\psi : \mathbb{R}^n \rightarrow \mathbb{R}$ be a convex function, and define

$$D_\psi(x, y) := \psi(x) - \nabla\psi(y)^\top x, \quad x, y \in \mathbb{R}^n.$$

The group divergence function can then be defined by

$$h_g(\beta) := D_\psi(\eta_g(\beta), Y_g), \quad \beta \in \mathbb{R}^p,$$

where $\eta_g(\beta) = X_g\beta$ is the linear predictor in group g . Note that as ψ is convex it follows that D_ψ , like the Bregman divergence, is convex in its first argument and in particular h_g is convex. However, unlike the Bregman divergence D_ψ is not non-negative.

A *general* soft maximin loss function $l_\zeta : \mathbb{R}^p \rightarrow \mathbb{R}$, is now given by

$$l_\zeta(\beta) := \text{lse}_\zeta \circ h(\beta) = \frac{\log(\sum_{j=1}^G e^{\zeta h_j(\beta)})}{\zeta}, \quad \zeta > 0,$$

and our aim is to solve the general soft maximin problem formulated as

$$\min_{\beta \in \mathbb{R}^p} l_\zeta(\beta) + \lambda J(\beta), \quad \lambda \geq 0. \quad (8)$$

Here J is a proper convex penalty function and λ is the penalty parameter.

Note that choosing ψ as the square norm yields the negative empirical explained variance $-\hat{V}_g$ as group divergence i.e. $h = -\hat{V}$. If $J = \|\cdot\|_1$, both loss and penalty are convex in this case, and (8) is equivalent to the (constrained) soft maximin problem (7) by strong Lagrangian duality. Hence in this case the solution to (8) is exactly the soft maximin estimator.

Solving (8) in a large scale setting requires an efficient optimization algorithm for non-differentiable problems. We note that when $h = -\hat{V}$, in contrast to the hard maximin problem, (8) is, in addition to convex and non-differentiable, also a separable problem (see Tseng and Yun (2009)) implying that the coordinate descent algorithm is viable. Here however, since we are particularly interested in solving (8) for data with array-tensor structure we are going to consider modified versions of the proximal gradient algorithm. As demonstrated in Lund et al. (2017) this algorithm is very well suited to handle this particular setup and can outperform the coordinate descent algorithm.

3.1 Solution algorithm

The proximal gradient algorithm fundamentally works by iteratively applying the proximal operator

$$\text{prox}_{\Delta J}(\beta) = \arg \min_{\gamma \in \mathbb{R}^p} \left\{ \frac{1}{2\Delta} \|\gamma - \beta\|_2^2 + J(\gamma) \right\}, \quad \Delta > 0 \quad (9)$$

to gradient based proposal steps. For a loss function with a Lipschitz continuous gradient with constant L , such an algorithm is guaranteed to converge to the solution as long as $\Delta \in (0, 2/L)$ making it attractive to obtain the smallest possible Lipschitz constant L .

With known L and fixed $\Delta \in (0, 2/L)$ a proximal gradient algorithm essentially consists of the following steps:

1. evaluate the gradient of the loss
2. evaluate the proximal operator $\text{prox}_{\Delta J}$
3. evaluate the loss function and penalty function.

The computational complexity in steps 1 and 3 is dominated by matrix-vector products, (see e.g. (4) for the soft maximin problem). The complexity in step 2 is determined by J . As noted in Beck and Teboulle (2009) when J is separable (e.g. the ℓ_1 -norm) $\text{prox}_{\Delta J}$ can be computed analytically or at low cost.

If L is not known (or if $\Delta \geq 2/L$ for a known, but perhaps conservative, L) we cannot guarantee convergence with a fixed choice of Δ , but adding a backtracking step will ensure convergence of the iterates. This extra step will increase the per-step computational cost of the algorithm.

When the gradient is not globally Lipschitz, it is no longer guaranteed that iterating steps 1-3 will yield a solution to (8) for any fixed Δ . However, we verify (Proposition 3) that the following non-monotone proximal gradient (NPG) algorithm, see Wright et al. (2009) and Chen et al. (2016), will converge to a solution of (8) under some regularity conditions.

Algorithm 1 NPG minimizing $F = f + \lambda J$

Require: $\beta^0, L_{\max} \geq L_{\min} > 0, \tau > 1, c > 0, M \geq 0$.

- 1: **for** $k = 0$ to $K \in \mathbb{N}$ **do**
 - 2: choose $L_k \in [L_{\min}, L_{\max}]$
 - 3: solve $\beta = \text{prox}_{\lambda J/L_k}(\beta^{(k)} - \frac{1}{L_k} \nabla f(\beta^{(k)}))$
 - 4: **if** $F(\beta) \leq \max_{[k-M]_+ \leq i \leq k} F(\beta^{(i)}) - c/2 \|\beta - \beta^{(k)}\|^2$ **then**
 - 5: $\beta^{(k+1)} = \beta$
 - 6: **else**
 - 7: $L_k = \tau L_k$ and go to 3
 - 8: **end if**
 - 9: **end for**
-

In particular, we show that while l_ζ does not have a Lipschitz continuous gradient in general, convergence of the NPG algorithm is still guaranteed under general conditions on the group functions h_1, \dots, h_G . Furthermore, in the special case where $h_g = -\hat{V}_g$ with all groups sharing the same design we show that l_ζ has a globally Lipschitz continuous gradient, and we derive a Lipschitz constant.

The first result states that l_ζ inherits strong convexity from any individual group divergence function h_g given that all h_1, \dots, h_G are convex and twice continuously differentiable. The proof is given in the appendix.

Proposition 2. For $g \in \{1, \dots, G\}$ assume h_g is twice continuously differentiable and

let $w_{g,\zeta}(\beta) := e^{\zeta h_g(\beta) - \zeta l_\zeta(\beta)}$, $\beta \in \mathbb{R}^p$. Then $(w_{j,\zeta}(\beta))_j$ are convex weights and

$$\nabla l_\zeta(\beta) = \sum_{j=1}^G w_{j,\zeta}(\beta) \nabla h_j(\beta) \quad (10)$$

$$\begin{aligned} \nabla^2 l_\zeta(\beta) &= \sum_{i=1}^G \sum_{j=i+1}^G w_{i,\zeta}(\beta) w_{j,\zeta}(\beta) (\nabla h_i(\beta) - \nabla h_j(\beta)) (\nabla h_i(\beta) - \nabla h_j(\beta))^\top \\ &\quad + \sum_{j=1}^G w_{j,\zeta}(\beta) \nabla^2 h_j(\beta). \end{aligned} \quad (11)$$

Furthermore if h_1, \dots, h_G are convex with at least one h_g strongly convex, then l_ζ and $e^{\zeta l_\zeta}$ are strongly convex.

Proposition 2 applies to the soft maximin loss with $h_g = -\hat{V}_g$. In this case $\nabla^2 h_g = 2\mathbf{X}_g^\top \mathbf{X}_g / n_g$, and h_g is strongly convex if and only if \mathbf{X}_g has rank p . Proposition 2 implies that if one of the matrices \mathbf{X}_g has rank p , l_ζ is strongly convex. However, we also see from Proposition 2 that $\nabla^2 l_\zeta(\beta)$ is not globally bounded in general. Consider the soft maximin loss, for instance, with $G = 2$, $p = n_1 = n_2 = 2$ and

$$\mathbf{X}_1 = \begin{pmatrix} 1 & 0 \\ 0 & 1 \end{pmatrix} \quad \text{and} \quad \mathbf{X}_2 = \begin{pmatrix} 0 & 0 \\ \sqrt{2} & 0 \end{pmatrix}. \quad (12)$$

Take also $y_1 = y_2 = 0$. When $\beta_1 = \beta_2 = r \in \mathbb{R}$ it holds that $h_1(\beta) = h_2(\beta) = r^2$ and thus $w_{1,\zeta} = w_{2,\zeta} = 1/2$ for any ζ , while

$$\begin{aligned} &(\nabla h_1(\beta) - \nabla h_2(\beta)) (\nabla h_1(\beta) - \nabla h_2(\beta))^\top \\ &= \begin{pmatrix} \beta_1^2 & -\beta_1 \beta_2 \\ -\beta_1 \beta_2 & \beta_2^2 \end{pmatrix} = \begin{pmatrix} r^2 & -r^2 \\ -r^2 & r^2 \end{pmatrix} \end{aligned}$$

is unbounded.

The following result shows, on the other hand, that for soft maximin estimation with identical \mathbf{X}_g -matrices across the groups, ∇l_ζ is, in fact, Lipschitz continuous. The proof is in the appendix.

Corollary 1. For each $g \in \{1, \dots, G\}$ let $\mathbf{X}_g = \mathbf{X}$ be a $m \times p$ matrix, \mathbf{Y}_g a $m \times 1$ vector and the group divergence given by

$$h_g(\beta) = \frac{1}{m} (2\beta^\top \mathbf{X}^\top \mathbf{Y}_g - \beta^\top \mathbf{X}^\top \mathbf{X} \beta).$$

Then ∇l_ζ has Lipschitz constant L bounded by

$$\frac{4}{m^2} \max_{i,j} \|\mathbf{X}^\top (\mathbf{Y}_i - \mathbf{Y}_j)\|^2 + \frac{2\|\mathbf{X}^\top \mathbf{X}\|}{m} \leq \frac{4\|\mathbf{X}^\top \mathbf{X}\|}{m^2} \left(\max_{i,j} \|\mathbf{Y}_i - \mathbf{Y}_j\|^2 + \frac{m}{2} \right), \quad (13)$$

with $\|\cdot\|$ the matrix norm induced by the 2-norm $\|\cdot\|$.

By Corollary 1 if we have identical designs across groups we can obtain the soft maximin estimator by applying the fast proximal gradient algorithm from Beck and Teboulle (2009) to the optimization problem (8). Furthermore in this setting the corollary gives an explicit expression for Lipschitz constant that will yield an efficient step size Δ for the solution algorithm.

Furthermore for soft maximin estimation with identical design across groups a standard version of this algorithm will solve the problem. This is particularly convenient in the array-tensor setup described next where the bound (13) is easy to compute. Note that the bound on the right hand side of (13) may be easier to compute as it avoids the matrix vector product. Also not that in this setup this bound can also be used to fix L_{min} in Algorithm 1.

Finally, in the general setup the following proposition shows that Algorithm 1, which does not rely on a global Lipschitz property (Chen et al. (2016)), solves the problem (8) given the assumptions in Proposition 2. The proof of the proposition is given in the appendix.

Proposition 3. *Assume h_1, \dots, h_G satisfy the assumptions in Proposition 2. Let $(\beta^{(k)})_k$ be a sequence of iterates obtained by applying the NPG algorithm to (8). Then $\beta^{(k)} \rightarrow \beta^*$ where β^* is a critical point of $l_\zeta + \lambda J$.*

In summary given a strongly convex group divergence function, e.g. satisfied in the soft maximin setup when one X_g has full rank, we can always solve the general problem (8) using a proximal gradient based algorithm.

3.2 Array tensor smoothing

As a leading example we will use soft maximin estimation in a setting where the objective is to extract a common signal from heterogeneous array data organized in G known groups. By array data we mean data with a geometry such that it is most naturally organized in a multidimensional array, as opposed to an unstructured vector. Canonical examples are images, movies, etc..

To formalize this data setting and model consider a regular grid in \mathbb{R}^d i.e. a d -dimensional lattice

$$\mathcal{Z}_1 \times \mathcal{Z}_2 \times \dots \times \mathcal{Z}_d \quad (14)$$

where $\mathcal{Z}_j = \{z_{j,1}, \dots, z_{j,m_j}\} \subset \mathbb{R}$ with $m_j \in \mathbb{N}, j \in \{1, \dots, d\}$. Let $m := \prod_{j=1}^d m_j$. If for each group g data $y_{g,1}, \dots, y_{g,m}$ is sampled across all points in (14) it may be organized in a fully populated d -dimensional $m_1 \times \dots \times m_d$ -array

$$\mathbf{Y}_g = (y_{g,i_1, \dots, i_d})_{i_1, \dots, i_d}, \quad i_j = 1, \dots, m_j, \quad j = 1, \dots, d. \quad (15)$$

For this reason we refer to this type of data as array data.

Preserving the array structure when formulating a multivariate smoothing model in this data setting leads to the array model equation

$$Y_{g,i_1, \dots, i_d} = f_g(z_{1,i_1}, \dots, z_{d,i_d}) + \epsilon_{g,i_1, \dots, i_d}, \quad z_{j,i_j} \in \mathcal{Z}_j, \quad (16)$$

for each $g \in \{1, \dots, G\}$, where f_g is a smooth group signal and $\epsilon_{g,i_1, \dots, i_d}$ an appropriate error term.

To obtain a linear array model from (16) we parameterize f_g using a basis expansion. A particularly convenient way of representing a multivariate function, is to use the tensor product construction to specify multivariate basis functions in terms of (tensor) products of families of univariate basis functions $((\varphi_{j,k})_{k=1}^{\infty})_{j=1}^d$. That is with $\varphi_{j,k} : \mathbb{R} \rightarrow \mathbb{R}$ the k th basis function in the j th dimension (k th j -marginal basis function) we represent the smooth signal as

$$f_g(z_1, \dots, z_d) = \sum_{k_1, \dots, k_d} \Theta_{g, k_1, \dots, k_d} \prod_{j=1}^d \varphi_{j, k_j}(z_j), \quad z_j \in \mathbb{R}, \quad (17)$$

where $(\Theta_{g, k_1, \dots, k_d})_{k_1, \dots, k_d}$ are basis coefficients.

Now, in order to implement this representation for the model (16) we need to determine the number of basis functions to use in the j th dimension, $p_j \in \mathbb{N}$, to obtain an (finite) approximation of f_g . For tensor product basis functions it is customary to choose p_j as a function of the cardinality of \mathcal{Z}_j e.g. $p_j = \lceil m_j/5 \rceil$ (see Currie et al. (2006)).

With $p_j \in \mathbb{N}$ fixed for each $j \in \{1, \dots, d\}$ we obtain the model (16) as a linear array model in the following way. For each $j \in \{1, \dots, d\}$ define a $m_j \times p_j$ matrix $\Phi_j = (\varphi_{j,k}(z_{j,i}))_{i,k}$ containing the values of the p_j basis functions evaluated at the m_j points in \mathcal{Z}_j . We call Φ_j a marginal design matrix. Also define a $p_1 \times \dots \times p_d$ -array $\Theta_g = (\Theta_{g, j_1, \dots, j_d})_{j_1=1, \dots, p_1, \dots, j_d=1, \dots, p_d}$ containing the corresponding basis coefficients.

It then follows directly from the identity (17) that the tensor (Kronecker) product of these marginal design matrices,

$$\Phi = \Phi_d \otimes \dots \otimes \Phi_2 \otimes \Phi_1, \quad (18)$$

is the design matrix for the linear model version of (16). This means that we can in principle implement (16) as a standard linear model using Φ . However from a computational complexity perspective that is suboptimal and potentially not feasible in large scale data settings as Φ grows as $\prod p_j \prod m_j$.

Instead, we can exploit the array tensor structure of the problem and only rely on the much smaller marginal matrices. As shown in Currie et al. (2006) any linear model with array structured data (15) and tensor structured design (18) can be formulated as a linear array model and fitted using so-called array arithmetic. The key computation is the rotated H -transform ρ , (see Currie et al. (2006) for details), that allows us to write the model (16) as a linear array model

$$\mathbf{Y}_g = \rho(\Phi_d, \rho(\Phi_{d-1}, \dots, \rho(\Phi_1, \Theta_g))) + \epsilon_g, \quad (19)$$

where ϵ_g is a $m_1 \times \dots \times m_d$ array containing the error terms.

As indicated by (19), using ρ the design matrix-parameter vector products, needed in steps 1 and 3 above, are computed without having access to the (very large) matrix Φ . In addition the computation has lower complexity than

the corresponding matrix-vector product (De Boor (1979), Buis and Dyksen (1996)).

Finally, the tensor structure in (18) makes the constant L in Corollary 1 easy to compute, see (30) in Lund et al. (2017). The implication is that we can run the proximal gradient algorithm without performing any backtracking.

Following Lund et al. (2017) we have implemented both a fast proximal algorithm as well as an NPG algorithm in a way that exploits the array-tensor structure described above. These implementations are available for 1D, 2D, and 3D array data in the R package *SMMA*, Lund (2020). The result is a computationally efficient numerical procedure that solves the soft maximin problem (8), while maintaining a small memory footprint.

4 Numerical experiments

We demonstrate the soft maximin method by setting up a prediction experiment for the model described in Section 3.2. The experiment is carried out on both a simulated data set as well as on the real neurological data and allows us to demonstrate properties of our methodology and compare these with those of existing methods. In particular the experiment aims at highlighting the role played by the soft maximin parameter ζ .

Specifically we benchmark performance against existing methods in terms of prediction accuracy, quantified by mean squared prediction error (MSPE) defined as $\|\hat{Y}_{x,s} - Y_{-s}\|_2^2$ where $\hat{Y}_{x,s}$ is the prediction from training on set s using method x and Y_{-s} are the observations in the complement to s . Furthermore we also bench computational complexity quantified by the observed run time. In addition we note that for the simulated data set we can explicitly compare the estimated common signal with the ground truth. Such comparison is not possible for the neuronal data. However given experimental setup that produced the neuronal data, and relying on neuroscientific concepts, basic features of the common response signal are known. A well estimated response signal should reflect these features.

The numerical experiment is in principle structured like K -fold cross validation aimed at discerning the optimal choice of hyperparameters ζ and λ in a grid search. Specifically by partitioning the groups in K subsets (folds) we train all methods, using the same λ and design, on one fold at the time and then compute test metrics on the remaining folds. We repeat this procedure N times to obtain NK fitted models and corresponding test metrics for each method.

For the penalty parameter λ we determine $M = 15$ values such that model no. 1 across all folds and methods is the zero model (no active features) and model no. 15 is sufficiently complex to capture any relevant features. We use this λ sequence for all folds and methods.

To evaluate the performance of the soft maximin estimator as a function of the parameter ζ we train the model for $\zeta = 2, 100, 200$. We also compute the pooled estimator corresponding to $\zeta = 0$ and the magging estimator from

Bühlmann and Meinshausen (2016). Magging is approximately (hard) maximin estimation and should therefore correspond roughly to $\zeta = \infty$.

We train the model using the same λ and design for all five methods. This in turn entails solving five different ℓ_1 -penalized estimation problems:

- To obtain the three soft maximin estimators we need to solve the problem (8) with ℓ_1 -norm penalty for each $\zeta = 2, 100, 200$. To do this we use the R package SMMA, Lund (2020).
- With identical (fixed) design across groups, we obtain the (penalized) pooled estimator by (penalized) regression of the empirical average across groups, on the fixed design. We use the R package glamlasso, Lund (2018) to solve the resulting Lasso problem.
- For the magging estimator we have to solve a Lasso problem for each group, given λ and the design. We use the R package glamlasso, Lund (2018) to obtain the individual group fits. These fits are then maximin aggregated (magging) across groups by solving a quadratic optimization problem as proposed in Bühlmann and Meinshausen (2016).

All computations are carried out on a Macbook Pro with a 2.8 GHz Intel core i7 processor and 16 GB of 1600 MHz DDR3 memory.

4.1 Simulated array data

We simulate data with three components: i) a common Gaussian signal of interest $\phi(x, y, t) = 200\phi_{12.5,4}(x)\phi_{12.5,4}(y)\phi_{50,25}(t)$ (ϕ_{μ,σ^2} is the density for the $\mathcal{N}(\mu, \sigma^2)$ distribution) superimposed with ii) periodic group specific signals with randomly varying frequency and phase and iii) additive white noise. Specifically for each $g \in \{1, \dots, G\}$ the 3-dimensional data array was simulated according to

$$Y_{g,i,j,k} = \phi(x_i, y_j, t_k) + 5 \sum_{j \in J_g} \varphi_j(x_i + p_g) \varphi_j(y_j + p_g) \varphi_j(t_k + p_g) + \epsilon_{g,i,j,k}, \quad (20)$$

with $x_i = 1, 2, \dots, 25$, $y_j = 1, 2, \dots, 25$ and $t_i = 1, 2, \dots, 101$. Here J_g is a set of 7 integers sampled uniformly from $\{1, \dots, 101\}$, φ_j is the j th Fourier basis function, $p_g \sim \text{unif}(-\pi, \pi)$, and $\epsilon_{g,i,j,k} \sim \mathcal{N}(0, 10)$.

We note that the common 3-dimensional Gaussian signal ϕ , due to its light tails, is spatially as well as temporally localized.

Figure 3 shows the simulated signals for three different groups plotted across time for $(i, j) = (12, 12)$. The common signal is dominated by group specific fluctuations in each group and not visually apparent.

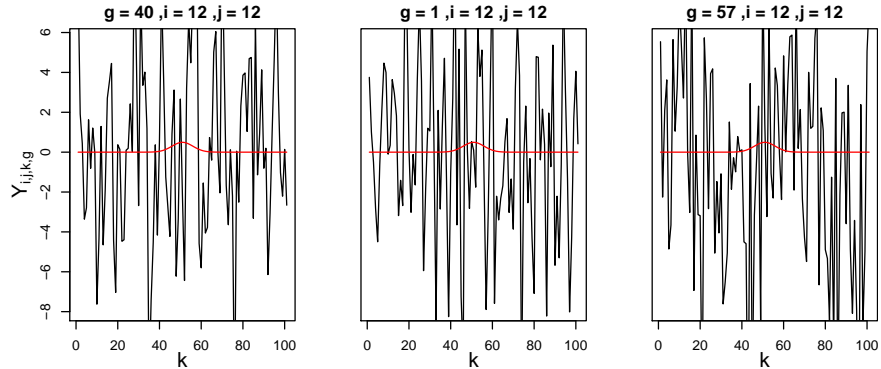


Figure 3: Temporal plot of the simulated data (black) for three different groups and the underlying common Gaussian signal (red).

4.1.1 Experiment setup

We use the array-tensor model from Section 3.2 with B-splines as basis functions in each dimension. The number of basis functions used in each dimension is respectively, $p_1 = p_2 = 10$ (spatial) and $p_3 = 23$ (temporal). This gives us an array model with marginal design matrices Φ_1 , Φ_2 , and Φ_3 , of size 25×10 , 25×10 , and 101×23 respectively, given by B-spline function evaluations over the marginal domains. The model has a total of 2300 parameters.

To set up the experiment we simulate $G = 100$ groups of 3-dimensional signals according to (20). We then randomly sample $K = 7$ folds (14 groups in each fold). This gives us a total of 883,750 observations in each fold.

For each method we train the model on each fold and test on the remaining 6 folds. By repeating this procedure $N = 10$ times we obtain 70 fits and corresponding test metrics for each method and each setting of λ .

4.1.2 Experimental results

The left display in Figure 4 shows the average of the mean squared error on the test sets, as a function of model complexity, i.e. each value of λ (model no.), for each method. The dashed line represents the average error made when using the zero signal, the most conservative estimate. The black line on the other hand is the average error when using the true signal as predicted values and is the optimal prediction for this data. We see the best performing method is the soft maximin with $\zeta = 200$ (red) while the worst is the pooled estimator (blue). In particular, the pooled estimator performs no better than the zero prediction. Surprisingly the magging estimator (yellow) does not perform much better than the zero prediction on average.

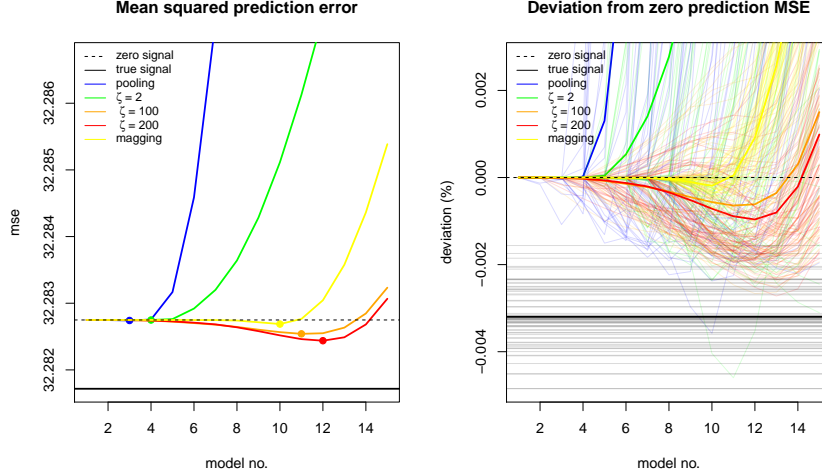


Figure 4: Left: Average MSE across 70 test sets as a function of model complexity (model no.). Zero signal (dashed), true signal (black), pooled estimator (blue), soft maximin $\zeta = 2$ (green), soft maximin $\zeta = 100$ (orange), soft maximin $\zeta = 200$ (red) and magging (yellow). The minimum is indicated with a bullet. Right: Deviation in MSE relative to the zero prediction MSE (percentage difference) for each method and on each test set (thin lines), as a function of model complexity. The corresponding averages are indicated with a thick line of the same color.

The right display in Figure 4 illustrates the variability in prediction accuracy for the different methods using their relative deviation in MSE from that of the zero prediction. The low ζ estimators (pooled and $\zeta = 2$) display high variability, reflecting a tendency to overfit group specific signals in the data. The high ζ soft maximin estimators and magging show much less variability. This underlines the robustness of the estimation methodology.

We note that while the gain in prediction performance, relative to the zero prediction is small, due to the low signal to noise ratio, it is not insignificant in terms of the quality of the extracted signal as illustrated in Figure 1. Here, the fit on four different training sets are displayed, and we observe directly how the low ζ methods tend to fit group fluctuation compared to the high ζ methods.

We quantify this by computing the mean squared signal error $\|\hat{Y}_{x,s} - \phi\|_2^2$ made by the prediction from training on set s using method x . The left display in Figure 5 shows the result for each method x and set s as a function of model complexity as well as the average over test set s and confirms the impression from Figure 1 and Figure 4.

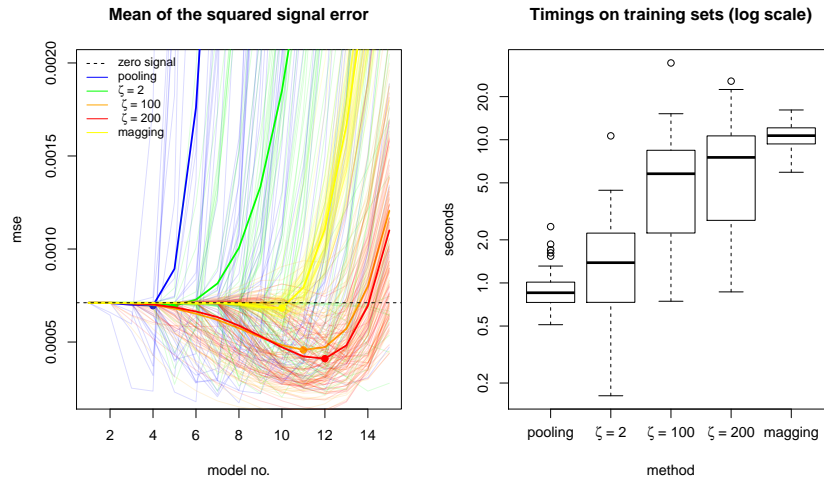


Figure 5: Left: mean squared signal error based on each of the 70 training set. Pooled estimator (blue), soft maximin $\zeta = 2$ (green), soft maximin $\zeta = 100$ (orange), soft maximin $\zeta = 200$ (red) and magging (yellow). Right: Summary of run times (log scale) for the 70 training sets for each method.

We note that only the high ζ methods succeed in extracting a common signal that is significantly more accurate than the zero prediction.

Finally, the right display in Figure 5 shows how each method performs in terms of run time. In this setting given the average response across the 14 groups in a fold, computing the pooled estimator has the same complexity as computing one group fit in the magging procedure. Not surprisingly the pooled estimator (0.9 s) is roughly 12 times faster than magging (10.7 s), and also roughly 6 to 7 times faster than the high ζ methods (6.1 s resp. 7.6 s). However, we note that compared to the soft maximin estimator with $\zeta = 2$ (1.7 s) the pooled least square estimator is not markedly faster.

4.2 Brain imaging data

The neuronal activity recordings were obtained using voltage-sensitive dye imaging (VSDI) in an experiment previously described in Roland et al. (2006). In short part of the visual cortex of a live ferret was exposed and stained with a voltage-sensitive dye. Any change in neuron cell membrane potential affects the dye and alters its fluorescence. In this way the neuronal activity is recorded indirectly in terms of changes in the fluorescence of the emitted light. The emitted light was recorded as an image using 464 photodiode channels organized in a two-dimensional (hexagonal) array. For the purpose of our analysis, the 464 channels were mapped to a 25×25 array yielding an image with 625 pixels, 161 of which contains no values. During the entire trial (625 ms) an image

was recorded every 0.6136 ms and for 250 ms of the trial a visual stimulus, a white square on a grey screen, was presented to the ferret. In the experiment a total of $G = 275$ trials (groups) were recorded across 13 different ferrets.

Several sources of heterogeneity are potentially present in the raw data:

1. The heart beat affects the light emission by expanding the blood vessels in the brain, creating a cyclic heart rate dependent artefact. A changing heart rate over trials for one animal (fatigue) as well as differences in heart rate between animals will cause heterogeneity in the data.
2. Spatial inhomogeneities can arise due to differences in the cytoarchitectural borders between the animals causing misalignment problems.
3. The VSDI technique is very sensitive, see Grinvald and Bonhoeffer (2002). Even small changes in the experimental surroundings could affect the recordings and create heterogeneity.
4. Differences between animals in how they respond to the visual stimulus.

A trial with no visual stimulus (baseline), was recorded right before recording the stimulus trial. By aligning the baseline and stimulus trial, using an electrocardiography recording, the two recordings were subtracted to remove the heart rate artefact. We use this preprocessed data in the experiment.

Figure 6 shows recordings for five trials in the temporal dimension (panel A) and spatial dimension (panel B). Note that following the onset of the visual stimulus after 200 ms (first dashed line), the recordings are expected to show the result of a depolarization of the neuronal cells. Visual inspection of Figure 6 however does not reveal a clear stimulus response in every trial. We note the presence of variation that seems to be specific to the trial and could reflect the heterogeneity listed above.

4.2.1 Experiment setup

We use the array-tensor model from Section 3.2 with $p_1 = p_2 = 9$ B-spline functions in each spatial dimension and $p_3 = 80$ B-splines in the temporal dimension. This gives us a linear array model with marginal design matrices Φ_1 , Φ_2 , and Φ_3 , of sizes 25×9 , 25×9 and 977×80 respectively, given by the B-splines evaluations over the marginal domains. The resulting model has a total of $p = 6480$ parameters.

In this numerical experiment we let one fold consist of all data from 2 out of the 13 animals. The model is trained on the fold and tested on all data from the remaining 11 animals, for each method and each value of λ . We repeat this procedure $N := \binom{13}{2} = 78$ times, yielding 78 fitted models and corresponding test metrics for each method and each value of λ . Since the number of trials is not constant across animals the number of groups in each fold ranges from 23 to 80 (average is 42) giving us 14,044,375 to 48,850,000 (average 25,646,250) observations in each fold.

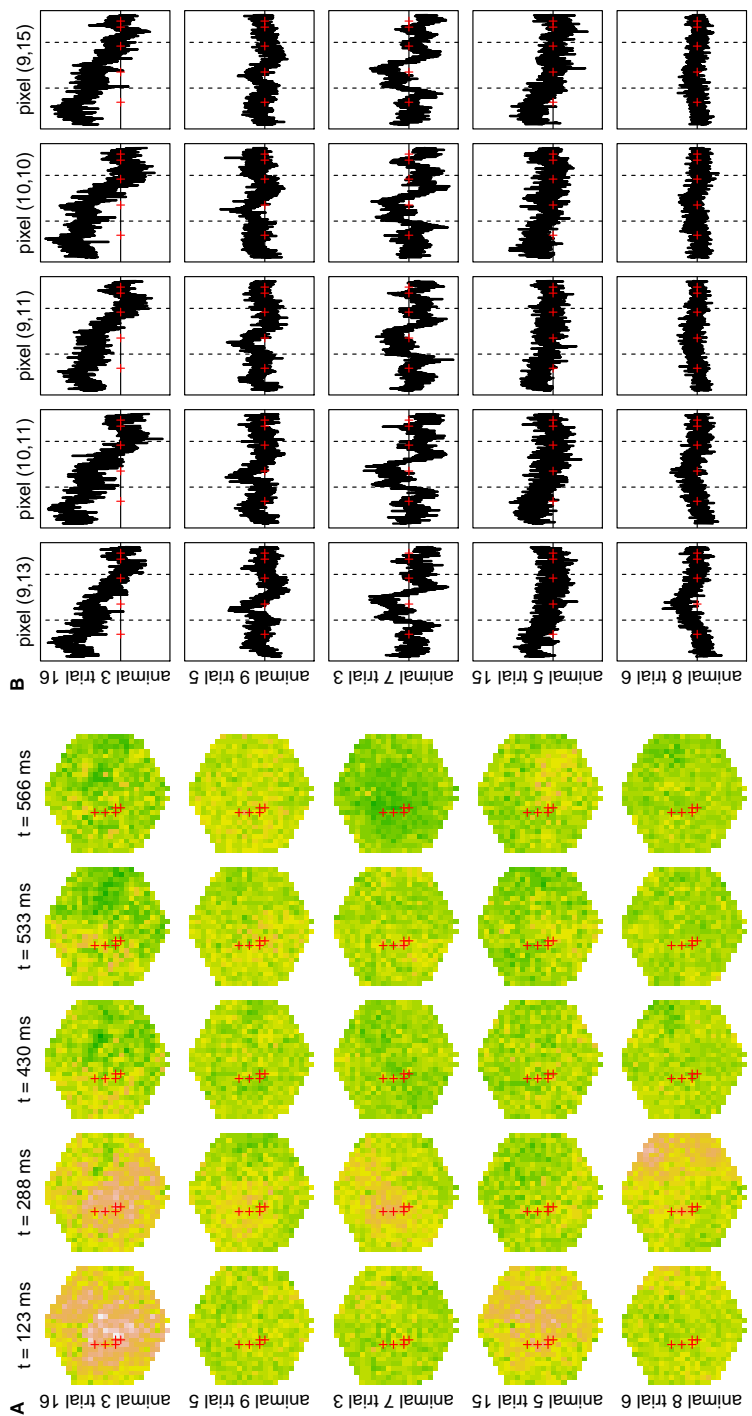


Figure 6: A: Spatial plots for five trials and five time points. The red crosses indicate the pixel time series shown in B. B: Temporal plots for the five same trials and five pixels indicated with red crosses in part A. The dashed lines indicate stimulus start and stop and red crosses indicate the time points plotted in part A.

4.2.2 Experimental results

From the left display in Figure 7 we see that on average soft maximin with $\zeta = 200$ (model no. 6) achieves the lowest over all out of sample MSE. The low ζ estimators, pooled (model no. 5) and $\zeta = 2$ (model no. 5) perform somewhat worse on average but still achieves significant reduction compared to the zero prediction. The approximate maximin estimator, magging estimator (model no. 13), performs the worst on this data in terms of MSE.

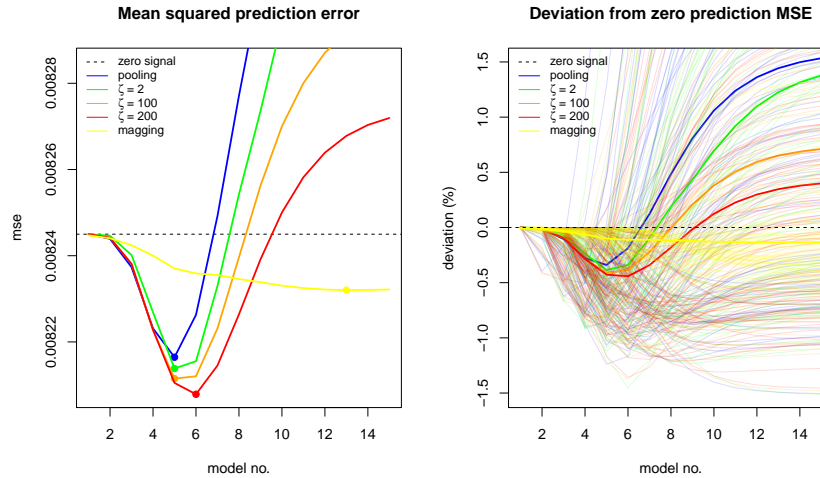


Figure 7: Left: Average MSE across 78 test sets as a function of model complexity (model no.). Zero signal (dashed), pooled estimator (blue), soft maximin $\zeta = 2$ (green), soft maximin $\zeta = 100$ (orange), soft maximin $\zeta = 200$ (red) and magging (yellow). The minimum is indicated with a bullet. Right: Deviation in MSE relative to the zero prediction MSE (percentage difference) for each method and on each test set (thin lines), as a function of model complexity. The corresponding averages are indicated with a thick line of the same color.

Looking at the right panel the low ζ methods show more variability than the high ζ methods and in particular are more prone to making predictions that are worse than the zero prediction. However the picture is not as clear as on the simulated data. We note that the magging estimator is quite consistently better than the zero prediction but not much, possibly reflecting the conservative nature of the hard maximin method.

Figure 8 summarizes the timings for each method. Notably all the soft maximin estimators (8.9 s, 15.8 s and 18.7 s) outperform the pooled estimator (26.4 s) while also yielding better prediction accuracy (Figure 7). The magging estimator (931.4 s) suffers from having to compute individual fits for each group in the training set, making the the method orders of magnitudes slower in

this case, without obtaining better accuracy. Note that the task alone of maximin aggregating the individual group estimates, by solving the associated quadratic programming problem, took on average 45 s. So even if fully parallelized the magging estimator is still computationally more demanding than the softmaximin estimator on this data set.

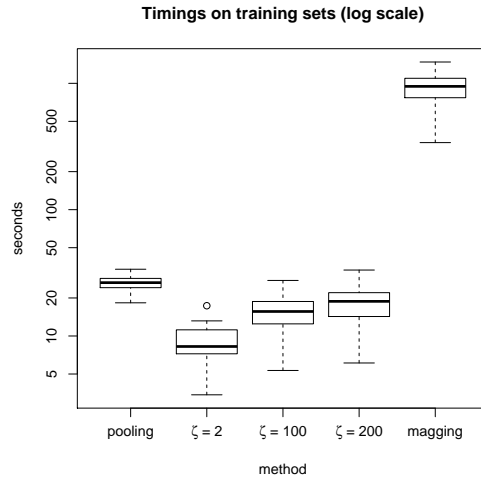


Figure 8: Summary of run times (log scale) for the 78 training sets for each method.

4.2.3 Response signal

We end by evaluating the response signal estimated by each method using the data from all $G = 275$ trials. When fitting the data for each method, we use the λ giving the lowest MSE from Section 4.2.2 for that particular method.

Figures 9 reveals that the pooled estimator and the soft maximin methods on the entire data set yield a similar estimated response signal. In particular a clear response to stimulus presentation (on signal), peaking after 288 ms, is picked up by all four methods. However, only the high ζ ($\zeta = 100, 200$) methods pick up a (slight) response to the visual stimulus being removed (off-signal), peaking after 533 ms. Note that the on-peak and off-peak occur with roughly the same delay relative to resp. stimulus presentation and stimulus removal (88 ms delay resp. 83 ms delay).

The methods also agree on spatial location in the visual cortex of the stimulus response signal, corresponding to the mapping of the center of field of view onto the visual cortex. A more spatially localized signal is obtained for $\zeta = 100, 200$.

The magging estimate of the response signal on the other hand hand is much more noisy and the stimulus response is less clear. Qualitatively it also

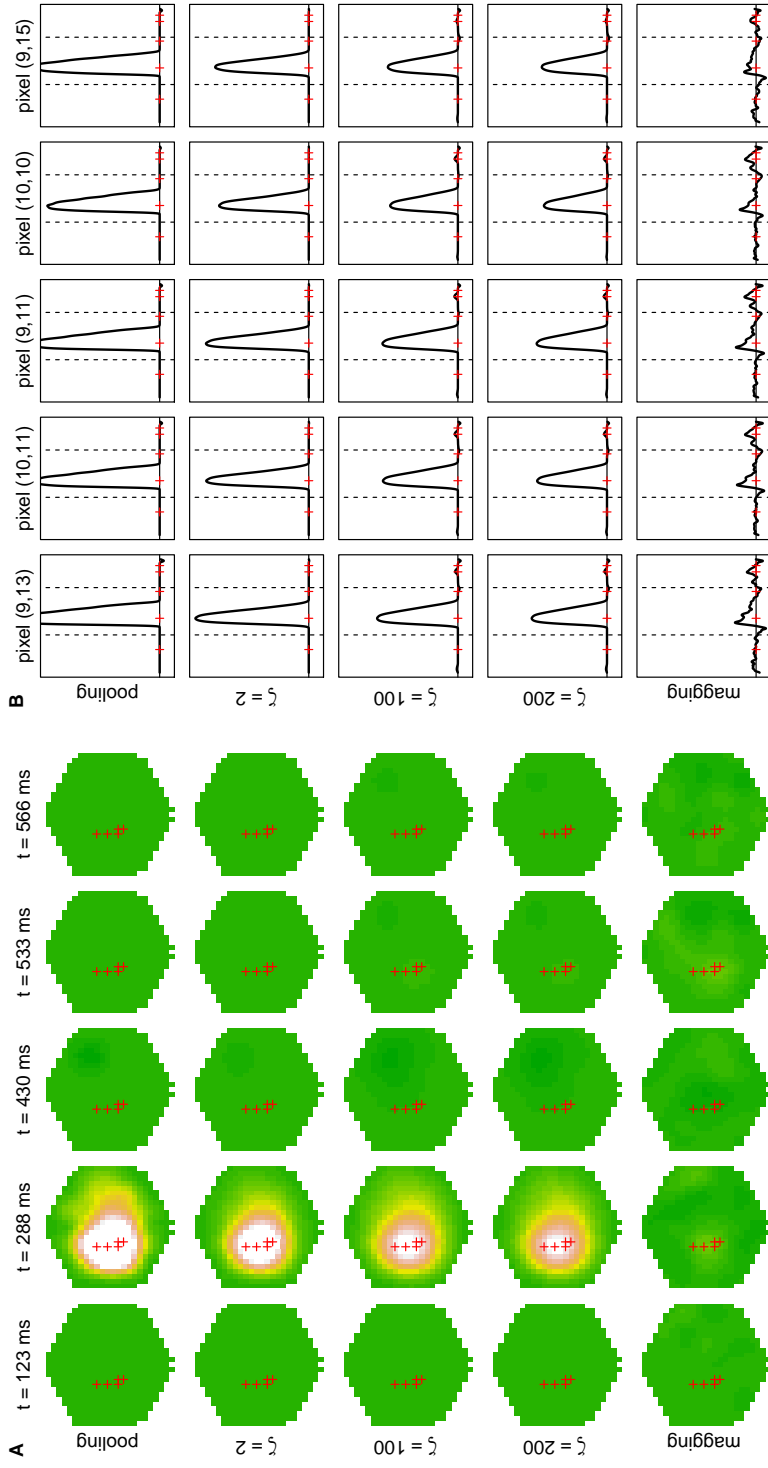


Figure 9: A: Spatial estimates for five different time points using all 275 trials from all animals as training data. From the top: pooled estimate, model no. 5; soft maximin, $\zeta = 2$, model no. 5; soft maximin, $\zeta = 100$, model no. 5; soft maximin, $\zeta = 200$, model no. 6; magging, model no. 13. The red crosses indicate the pixels plotted as timeseries in part B. B: The corresponding temporal estimates, for the five different pixels indicated with red crosses in part A. The dashed lines indicate stimulus start and stop and red crosses indicate the time points plotted in part A.

looks differently with less difference between the on peak and off peak.

We conclude, that on this data set the softmaximin method outperforms both pooling and magging methods both in terms of prediction error and runtime. However the difference in prediction error, between the softmaximin methods and pooling, is not very pronounced as also illustrated by the similarity in the estimated response signal. This reflects that while very noisy, the neuron data has, perhaps surprisingly, a fairly similar response signal in all trials (groups), with apparently little systematic group variation and heterogeneity.

5 Discussion

The maximin estimator with the ℓ_1 -penalty, as defined in Meinshausen and Bühlmann (2015), solves the minimization problem

$$\hat{\beta}_{mm} := \arg \min_{\beta} \max_g \{-\hat{V}_g(\beta)\} + \lambda \|\beta\|_1. \quad (21)$$

Though the objective function is convex, it is nondifferentiable as well as non-separable, and contrary to the claim in Section 4 of Meinshausen and Bühlmann (2015), coordinate descent will not always solve (21).

Two approximate approaches for solving (21) were suggested in Meinshausen and Bühlmann (2015). The first, also a smooth approximation of the term $\max_g \{-\hat{V}_g(\beta)\}$, however, appears theoretically invalid and we did not find it to work in practice either. The second approximation, the maximal penalty solution, obtains a solution to (21) for the maximum λ that yields a non-zero solution (at least one active feature) to (21). This solution is appropriate as an efficient initial estimator and clearly much cruder than a fine tuned maximin estimator.

We note in passing that the solution path of (21) is piecewise linear in λ , and it may thus be computed using a method like LARS, see Roll (2008). A LARS-type algorithm or a coordinate descent algorithm of a smooth majorant, such as the soft maximin loss, has subsequently also been proposed to us by Meinshausen (personal communication) as better alternatives to those suggested in Meinshausen and Bühlmann (2015). In our experience, the LARS-type algorithm scales poorly with the size of the problem, and neither LARS nor coordinate descent can exploit the array-tensor structure.

Magging, as proposed in Bühlmann and Meinshausen (2016) as yet another alternative to (21) for estimation of maximin effects, is also computationally straightforward, but as we demonstrated in the numerical experiment not computationally faster than using the soft maximin estimator. We note that in our experiment we did not parallelize computations which if done efficiently could benefit magging greatly in terms of runtime. However as noted just computing the maximin aggregation, i.e. solving the quadratic programming problem, is still more time consuming than the computing the soft maximin estimate for the neuron data.

The numerical experiments also showed magging trailing soft maximin estimation in terms of predictive performance. It was demonstrated both on simulated and the neuronal VSDI data how the soft maximin estimator was able to extract a signal, in the context of multivariate array data, and how the choice of the tuning parameter ζ affects the extracted signal and the prediction performance. In particular the simulations showed that soft maximin estimation ($\zeta = 100, 200$) can extract a signal even in the presence of large heterogeneous noise components where the other methods failed

We have developed soft maximin estimation as an alternative to maximin estimation that retains desirable statistical properties and is computationally more efficient. From the definition of the soft maximin loss the intention of ζ is to control the tradeoff in the estimation between groups with large explained variance and groups with small explained variance. The gradient representation (10) shows explicitly how this tradeoff works in the NPG algorithm: the gradient of the soft maximin loss is a convex combination of the gradients of the group-wise loss functions with weights controlled by ζ . The largest weights are on those groups with the smallest explained variances and as $\zeta \rightarrow \infty$ the weights concentrate on the groups with minimal explained variance.

Thus our proposed algorithm provides a means for approximately minimizing (21) and is as such an alternative to magging as an estimator of the maximin effect. More importantly, by the introduction of the tuning parameter ζ in the soft maximin loss we not only achieved an approximate solution of (21) but an interpolation between the (hard) maximin estimator and the pooled WLS estimator.

The R package *SMMA*, Lund (2020), provides an implementation of our method for models with identical design across groups e.g. as in section 3.2. Here the context of large-scale spatio-temporal (array) data offers potential applications. One example is provided by the climate models in the Coupled Model Inter-comparison Project (CMIP). These models produce different (heterogenous) predictions for the same spatio-temporal surface (earth over time). By applying the model setting from Section 3.2, it might be possible to obtain an improved model consensus estimate, using the soft-maximin estimator (see e.g. Sander-son et al. (2017)).

We expect that soft maximin estimation will be practically useful in a number of different contexts, as a way of aggregating explained variances across groups. In particular because it downweights groups with a large explained variance that might simply be outliers, while it does not go to the extreme of the maximin effect, that can kill the signal completely.

A Proofs

Proof of Lemma 1. i) Since $x_g = \max\{x_1, \dots, x_G\}$ for some $g \in \{1, \dots, G\}$,

$$\max\{x_1, \dots, x_G\} = \frac{\log(e^{\zeta x_g})}{\zeta} \leq \frac{\log(e^{\zeta x_g} + \sum_{j \neq g} e^{\zeta x_j})}{\zeta} = \text{lse}(x)$$

and also

$$\text{lse}(x) \leq \frac{\log(\sum_j e^{\zeta x_j})}{\zeta} = \frac{\log(Ge^{\zeta x_g})}{\zeta} = \frac{\log(G)}{\zeta} + \max\{x_1, \dots, x_G\},$$

and the statement follows.

ii) From l'Hopitals rule we get

$$\lim_{\zeta \downarrow 0} \frac{\log(\frac{1}{G} \sum_j e^{\zeta x_j})}{\zeta} = \lim_{\zeta \downarrow 0} \left(\frac{1}{G} \sum_j x_j e^{\zeta x_j} \right) \left(\frac{1}{G} \sum_j e^{\zeta x_j} \right)^{-1} = \frac{1}{G} \sum_j x_j,$$

implying

$$\text{lse}(x) = \frac{\log(G)}{\zeta} + \frac{\log(\frac{1}{G} \sum_j e^{\zeta x_j})}{\zeta} = \frac{\log(G)}{\zeta} + \frac{1}{G} \sum_j x_j + o(1),$$

for $\zeta \downarrow 0$. □

Proof of Proposition 1. First note that for any $\beta \in \mathbb{R}^p$ and any $g \in \{1, \dots, G\}$

$$\begin{aligned} -\hat{V}_g(\beta) &= \beta^\top \hat{\Sigma}_g \beta - 2\beta^\top \hat{\Sigma}_g b_g - \frac{2\beta^\top \mathbf{X}_g^\top \epsilon_g}{n_g} \\ &= -V_{b_g}(\beta) + \beta^\top (\hat{\Sigma}_g - \Sigma) \beta - 2\beta^\top (\hat{\Sigma}_g - \Sigma) b_g - \frac{2\beta^\top \mathbf{X}_g^\top \epsilon_g}{n_g} \\ &\geq -V_{b_g}(\beta) - \|\beta\|_1^2 D - 2\|\beta\|_1 \max_g \|b_g\|_1 D - 2\|\beta\|_1 \delta \end{aligned} \quad (22)$$

and correspondingly

$$-\hat{V}_g(\beta) \leq -V_{b_g}(\beta) + \|\beta\|_1^2 D + 2\|\beta\|_1 \max_g \|b_g\|_1 D + 2\|\beta\|_1 \delta. \quad (23)$$

By assumption $\max_g \|b_g\|_1 \leq \kappa$, and if also $\|\beta\|_1 \leq \kappa$ we can write

$$\text{lse}_\zeta(-V(\beta)) - 3\kappa^2 D - 2\kappa\delta \leq \text{lse}_\zeta(-\hat{V}(\beta)) \quad (24)$$

$$\leq \text{lse}_\zeta(-V(\beta)) + 3\kappa^2 D + 2\kappa\delta, \quad (25)$$

by (22) and (23) and the properties of lse_ζ .

Let H denote the convex hull of $\{b_1, \dots, b_g\}$. By Theorem 1 in Meinshausen and Bühlmann (2015) we know that $b^* \in H$ and since $\max_g \|b_g\|_1 \leq \kappa$ we also have $\|b^*\|_1 \leq \kappa$. By (7) it follows that

$$\text{lse}_\zeta(-\hat{V}(\hat{\beta}_{smm}^k)) \leq \text{lse}_\zeta(-\hat{V}(b^*)). \quad (26)$$

Using (24) and (25) on respectively the left and right hand side of (26), yields

$$\text{lse}_\zeta(-V(\hat{\beta}_{smm}^k)) \leq \text{lse}_\zeta(-V(b^*)) + 6\kappa^2 D + 4\kappa\delta. \quad (27)$$

Applying Lemma 1 on both left and right hand side of (27) finally yields

$$\max_g \{-V_{b_g}(\hat{\beta}_{smm}^\kappa)\} \leq \max_g \{-V_{b_g}(b^*)\} + 6\kappa^2 D + 4\kappa\delta + \frac{\log(G)}{\zeta}. \quad (28)$$

For the last statement, note that for fixed $\beta \in \mathbb{R}^p$, since $b \mapsto -V_b(\beta)$ is affine

$$\max_g \{-V_{b_g}(\beta)\} = \max_{b \in H} \{-V_b(\beta)\}. \quad (29)$$

An implication of Theorem 1 in Meinshausen and Bühlmann (2015) is $(b^*)^\top \Sigma b \geq (b^*)^\top \Sigma b^*$, $\forall b \in H$, which combined with (29) shows

$$\max_g \{-V_{b_g}(b^*)\} = \max_{b \in H} \{(b^*)^\top \Sigma b^* - 2(b^*)^\top \Sigma b\} = -(b^*)^\top \Sigma b^*. \quad (30)$$

Using $b^* \in H$ and (29), on the left hand side of (28), and using (30) on the right hand side of (28), gives us

$$(\hat{\beta}_{smm}^\kappa)^\top \Sigma \hat{\beta}_{smm}^\kappa - 2(\hat{\beta}_{smm}^\kappa)^\top \Sigma b^* \leq -(b^*)^\top \Sigma b^* + 6\kappa^2 D + 4\kappa\delta + \frac{\log(G)}{\zeta},$$

which can be rearranged to yield the statement. \square

To prove Proposition 2 we need the following technical lemma.

Lemma 2. Assume $\sum_i w_i = 1$ and $h_i \in \mathbb{R}^p$, $i \in \{1, \dots, G\}$, $G \in \mathbb{N}$. Then

$$\sum_i w_i h_i \left(h_i^\top - \sum_j w_j h_j^\top \right) = \sum_i \sum_{j>i} w_i w_j (h_i - h_j)(h_i - h_j)^\top.$$

Proof. First note that since $1 - w_i = \sum_{j \neq i} w_j$

$$\begin{aligned} \sum_i w_i h_i \left(h_i^\top - \sum_j w_j h_j^\top \right) &= \sum_i w_i h_i \left((1 - w_i) h_i^\top - \sum_{j \neq i} w_j h_j^\top \right) \\ &= \sum_i \sum_{j \neq i} w_i w_j h_i (h_i - h_j)^\top. \end{aligned}$$

Letting $a_{i,j} = w_i w_j h_i (h_i - h_j)^\top$ we find that

$$\begin{aligned} \sum_i \sum_{j \neq i} a_{i,j} &= \sum_i \sum_{j>i} a_{i,j} + \sum_i \sum_{i>j} a_{i,j} \\ &= \sum_i \sum_{j>i} a_{i,j} + \sum_j \sum_{i>j} a_{i,j} \quad (\text{interchange summation order}) \\ &= \sum_i \sum_{j>i} a_{i,j} + \sum_i \sum_{j>i} a_{j,i} \quad (\text{relabel summation indices}) \\ &= \sum_i \sum_{j>i} w_i w_j (h_i - h_j)(h_i - h_j)^\top, \end{aligned}$$

where we used that $a_{j,i} = -w_i w_j h_j (h_i - h_j)^\top$. \square

Proof of Proposition 2. First it is straightforward to compute the gradient of the loss

$$\begin{aligned}
\nabla l_\zeta(\beta) &= \frac{\sum_{j=1}^G e^{\zeta h_j(\beta)} \nabla \zeta h_j(\beta)}{\zeta \sum_{j=1}^G e^{\zeta h_j(\beta)}} \\
&= e^{-\log(\sum_{j=1}^G e^{\zeta h_j(\beta)})} \sum_{j=1}^G e^{\zeta h_j(\beta)} \nabla h_j(\beta) \\
&= \sum_{j=1}^G w_{j,\zeta}(\beta) \nabla h_j(\beta). \tag{31}
\end{aligned}$$

Then since

$$w_{j,\zeta}(\beta) = \frac{e^{\zeta h_j(\beta)}}{\sum_{i=1}^G e^{\zeta h_i(\beta)}} \geq 0$$

we see that $\sum_j w_{j,\zeta}(\beta) = 1$ and conclude that the weights $w_\zeta(\beta)$ are convex for any β and ζ .

Differentiating (31) gives us

$$\nabla^2 l_\zeta(\beta) = \sum_{j=1}^G \nabla h_j(\beta) \nabla w_{j,\zeta}(\beta)^\top + \sum_{j=1}^G w_{j,\zeta}(\beta) \nabla^2 h_j(\beta).$$

Using the definition of $w_{j,\zeta}$ and (31) the first term is equal to

$$\begin{aligned}
&\sum_{j=1}^G w_{j,\zeta}(\beta) \nabla h_j(\beta) \left(\nabla h_j(\beta)^\top - \sum_{i=1}^G w_{i,\zeta}(\beta) \nabla h_i(\beta)^\top \right) \\
&= \sum_{j=1}^G \sum_{i>j} w_{j,\zeta}(\beta) w_{i,\zeta}(\beta) (\nabla h_j(\beta) - \nabla h_i(\beta)) (\nabla h_j(\beta) - \nabla h_i(\beta))^\top
\end{aligned}$$

where the equality follows from Lemma 2 since $(w_{j,\zeta}(\beta))_j$ are convex weights.

For a twice continuously differentiable function f it holds that f is strongly convex with parameter $\nu > 0$ if and only if $\nabla^2 f - \nu I$ is positive semi definite. Assuming all h_i are convex and at least one is ν -strongly convex it follows directly from (11) that l_ζ is also ν -strongly convex.

Finally, the Hessian of $e^{l_\zeta(\beta)}$ is

$$\nabla^2 e^{l_\zeta(\beta)} = \nabla^2 l_\zeta(\beta) e^{l_\zeta(\beta)} + \nabla_\beta l_\zeta(\beta) \nabla_\beta l_\zeta(\beta)^\top e^{l_\zeta(\beta)}$$

where $\nabla_\beta l_\zeta(\beta) \nabla_\beta l_\zeta(\beta)^\top e^{l_\zeta(\beta)}$ is positive semi-definite for all β . Letting $m = \min_\beta l_\zeta(\beta) \in \mathbb{R}$, we have $e^{l_\zeta(\beta)} \geq e^m > 0$ for all β and must have $\nabla^2 e^{l_\zeta(\beta)} - \tilde{\nu} I$ is positive semi definite for some $\tilde{\nu} > 0$, showing that e^{l_ζ} is strongly convex. \square

Proof of Corollary 1. Let $\|\cdot\|_d$ denote the 2-norm on \mathbb{R}^d and A be a $d_1 \times d_2$ matrix. Then $\|A\|_{d_1, d_2} := \sup_{v: \|v\|_{d_2}=1} \|Av\|_{d_1}$ is the sub-multiplicative matrix (operator) norm induced by the 2-norms on \mathbb{R}^{d_1} and \mathbb{R}^{d_2} . For $a \in \mathbb{R}^{d_1}$ and $b \in \mathbb{R}^{d_2}$ note that $\|a\|_{d_1, 1} = \|a\|_{d_1}$ (Cauchy-Schwarz) and we get

$$\|ab^\top\| = \sup_{v: \|v\|_{d_2}=1} \|ab^\top v\|_{d_1} = \sup_{v: \|v\|_{d_2}=1} \|a\|_{d_1} |b^\top v| = \|a\|_{d_1} \|b\|_{d_2}.$$

Now suppressing subscripts observe that $\|\nabla^2 h_g(\beta)\| = 2\|\mathbf{X}^\top \mathbf{X}\|/m$ and $\nabla h_i(\beta) - \nabla h_j(\beta) = 2\mathbf{X}^\top (\mathbf{Y}_i - \mathbf{Y}_j)/m$. Then by Proposition 2 it follows that

$$\begin{aligned} \|\nabla^2 l_\zeta(\beta)\| &\leq \sum_i \sum_{j>i} w_{i,\zeta}(\beta) w_{j,\zeta}(\beta) \|(\nabla h_i(\beta) - \nabla h_j(\beta))(\nabla h_i(\beta) - \nabla h_j(\beta))^\top\| \\ &\quad + \sum_j w_{j,\zeta}(\beta) \|\nabla^2 h_j(\beta)\| \\ &= \frac{4}{m^2} \sum_i \sum_{j>i} w_{i,\zeta}(\beta) w_{j,\zeta}(\beta) \|\mathbf{X}^\top (\mathbf{Y}_i - \mathbf{Y}_j)\|^2 + \frac{2\|\mathbf{X}^\top \mathbf{X}\|}{m} \\ &\leq \frac{4}{m^2} \max_{i,j} \|\mathbf{X}^\top (\mathbf{Y}_i - \mathbf{Y}_j)\|^2 + \frac{2\|\mathbf{X}^\top \mathbf{X}\|}{m} \\ &\leq \frac{4\|\mathbf{X}^\top \mathbf{X}\|}{m^2} \left(\max_{i,j} \|\mathbf{Y}_i - \mathbf{Y}_j\|^2 + \frac{m}{2} \right) \end{aligned}$$

using the properties of the matrix norm. By the mean value theorem it follows that ∇l_ζ is Lipschitz continuous with the claimed bound. \square

Proof of Proposition 3. If we can show that Assumption A.1 from Chen et al. (2016) holds for the soft maximin problem (8) we can use Theorem A.1 in Chen et al. (2016) (or Lemma 4 in Wright et al. (2009)) to show that the sequence has an accumulation point. Theorem 1 in Wright et al. (2009) then establishes this accumulation point as a critical point for $F_\zeta = l_\zeta + \lambda J$.

Let $\Delta > 0$, $\beta_0 \in \mathbb{R}^p$, and define the set

$$\begin{aligned} A_0 &= \{\beta : F_\zeta(\beta) \leq F_\zeta(\beta_0)\} \\ A_{0,\Delta} &= \{\beta : \|\beta - \beta'\| \leq \Delta, \beta' \in A_0\}. \end{aligned}$$

A.1(i): l_ζ is ν -strongly convex by Proposition 2 and since J is assumed convex it follows that F_ζ is strongly convex. So A_0 is compact hence $A_{0,\Delta}$ is compact as a closed neighbourhood of A_0 . As l_ζ is C^∞ everywhere, ∇l_ζ is Lipschitz on $A_{0,\Delta}$.

A.1(ii): Is satisfied by assumptions on J .

A.1(iii): Clearly $F_\zeta \geq 0$. Furthermore F_ζ is continuous hence uniformly continuous on the compact set A_0 .

A.1(iv) $\sup_{\beta \in A_0} \|\nabla l_\zeta\| < \infty$ as A_0 is compact and ∇l_ζ is continuous. Moreover, $\sup_{\beta \in A_0} \|J\| < \infty$ as A_0 is compact and J is continuous. Finally, also $\inf J = 0$. \square

References

- Beck, A. and M. Teboulle (2009). A fast iterative shrinkage-thresholding algorithm for linear inverse problems. *SIAM Journal on Imaging Sciences* 2(1), 183–202.
- Bühlmann, P. and N. Meinshausen (2016). Magging: maximin aggregation for inhomogeneous large-scale data. *Proceedings of the IEEE* 104(1), 126–135.
- Buis, P. E. and W. R. Dyksen (1996). Efficient vector and parallel manipulation of tensor products. *ACM Transactions on Mathematical Software (TOMS)* 22(1), 18–23.
- Chen, X., Z. Lu, and T. K. Pong (2016). Penalty methods for a class of non-lipschitz optimization problems. *SIAM Journal on Optimization* 26(3), 1465–1492.
- Currie, I. D., M. Durban, and P. H. Eilers (2006). Generalized linear array models with applications to multidimensional smoothing. *Journal of the Royal Statistical Society: Series B (Statistical Methodology)* 68(2), 259–280.
- De Boor, C. (1979). Efficient computer manipulation of tensor products. *ACM Transactions on Mathematical Software (TOMS)* 5(2), 173–182.
- Grinvald, A. and T. Bonhoeffer (2002). Optical imaging of electrical activity based on intrinsic signals and on voltage sensitive dyes: The methodology.
- Lund, A. (2018). *glamlasso: Penalization in Large Scale Generalized Linear Array Models*. R package version 3.0.
- Lund, A. (2020). *SMMA: Soft Maximin Estimation for Large Scale Array-Tensor Models*. R package version 1.0.3.
- Lund, A., M. Vincent, and N. R. Hansen (2017). Penalized estimation in large-scale generalized linear array models. *Journal of Computational and Graphical Statistics* 26(3), 709–724.
- Meinshausen, N. and P. Bühlmann (2015). Maximin effects in inhomogeneous large-scale data. *The Annals of Statistics* 43(4), 1801–1830.
- Roland, P. E., A. Hanazawa, C. Undeman, D. Eriksson, T. Tompa, H. Nakamura, S. Valentiniene, and B. Ahmed (2006). Cortical feedback depolarization waves: A mechanism of top-down influence on early visual areas. *Proceedings of the National Academy of Sciences* 103(33), 12586–12591.
- Roll, J. (2008). Piecewise linear solution paths with application to direct weight optimization. *Automatica* 44(11), 2732–2737.
- Sanderson, B. M., M. Wehner, and R. Knutti (2017). Skill and independence weighting for multi-model assessments. *Geoscientific Model Development* 10(6), 2379–2395.

- Scheipl, F., A.-M. Staicu, and S. Greven (2015). Functional additive mixed models. *Journal of Computational and Graphical Statistics* 24(2), 477–501.
- Staicu, A.-M., C. M. Crainiceanu, and R. J. Carroll (2010). Fast methods for spatially correlated multilevel functional data. *Biostatistics* 11(2), 177–194.
- Tseng, P. and S. Yun (2009). A coordinate gradient descent method for nonsmooth separable minimization. *Mathematical Programming* 117(1-2), 387–423.
- Wang, J.-L., J.-M. Chiou, and H.-G. Müller (2016). Functional data analysis. *Annual Review of Statistics and Its Application* 3(1), 257–295.
- Wright, S. J., R. D. Nowak, and M. A. Figueiredo (2009). Sparse reconstruction by separable approximation. *IEEE Transactions on Signal Processing* 57(7), 2479–2493.